Evidence for fault lubrication during the 1999 Chi-Chi, Taiwan, earthquake (Mw7.6)

Kuo-Fong Ma,[1] Emily E. Brodsky,[2] Jim Mori,[3] Chen Ji,[4] Teh-Ru A. Song,[4] and Hiroo Kanamori[4]

[1] The ground motion data of the 1999 Chi-Chi, Taiwan, earthquake exhibit a striking difference in frequency content between the north and south portions of the rupture zone. In the north, the ground motion is dominated by large low-frequency displacements with relatively small high-frequency accelerations. The pattern is opposite in the south, with smaller displacements and larger accelerations. We analyze the fault dynamics in light of a fault lubrication mechanism using near-field seismograms and a detailed rupture model. The fault zone contains viscous material (e.g., gouge), in which pressure increases following the Reynolds lubrication equation. When the displacement exceeds a threshold, lubrication pressure becomes high enough to widen the gap, thereby reducing the area of asperity contact. With less asperity contact, the fault slips more smoothly, suppressing high-frequency radiation. *INDEX TERMS:* 7209 Seismology: Earthquake dynamics and mechanics; 7212 Seismology: Earthquake ground motions and engineering; 7215 Seismology: Earthquake parameters; *KEYWORDS:* Chi-Chi Taiwan earthquake, high slip velocity, near-field strong motion station, fault dynamics, fault lubrication, fluid pressurization. **Citation:** Ma, K.-F., E. E. Brodsky, J. Mori, C. Ji, T.-R. A. Song, and H. Kanamori, Evidence for fault lubrication during the 1999 Chi-Chi, Taiwan, earthquake (Mw7.6), *Geophys. Res. Lett.*, *30*(5), 1244, doi:10.1029/2002GL015380, 2003.

1. Introduction

[2] Recent kinematic and dynamic studies of the rupture process of large earthquakes have shed new light on the fundamental role of friction in fault mechanics [e.g., *Fukuyama and Madariaga*, 1998]. The September 20, 1999 (M_w 7.6) Chi-Chi, Taiwan, earthquake provided important new data from extensive strong-motion instrumentation for investigating the physics of faulting. The stations near the largest observed surface offset, near the northern end of Chelungpu fault, recorded large ground velocities and displacements (vectorial amplitudes of up to 4.5 m/s and 12 m, respectively). These are the largest values ever instrumentally measured. In contrast, the ground accelerations are higher in the southern part of the fault, even though the ground velocities and fault displacements are less than in the north, as shown in Figure 1. The relatively low level of high-frequency radiation along with the large slip velocities and displacements on the northern portion of the fault, as observed at stations TCU052 and TCU068, are at odds with the

observations for many large earthquakes. Here, we interpret, through examinations of near-field seismograms and a detailed rupture model, the fault dynamics of the 1999 Chi-Chi earthquake in light of a fault lubrication mechanism.

[3] *Brodsky and Kanamori* [2001] applied the theory of mechanical lubrication developed by *Sommerfeld* [1950] for journal bearings to earthquake faulting. If a fault zone is thin and slightly rough, and if the material in the fault zone behaves like a viscous fluid, then as the displacement and velocity of fault motion increase, the fluid pressure within the fault zone rises. The increased pressure (i.e., lubrication pressure) reduces friction; the lubrication pressure also elastically deforms the fault wall, widens the gap, and reduces the contact area between the asperities on the fault walls. This results in a reduction in high-frequency energy radiation produced by asperity collisions. If reduced levels of high frequency radiation associated with large slip are observed on faults in diverse geological settings, it is likely that dynamic processes, such as lubrication, plays a key role in dynamics of faulting. Although other mechanisms such as melting and fluid pressurization may have similar effects on rupture dynamics of the Chi-Chi earthquake, we will show that the predictions of lubrication are consistent with the observations, suggesting that the mechanical lubrication provides a plausible mechanism for fault dynamics of the Chi-Chi earthquake.

2. Waveforms at Station TCU068

[4] First, we show that the EW component seismograms recorded at station TCU068 (Figure 2) exhibit the behavior predicted by this lubrication mechanism. As shown in Figure 2, the acceleration, velocity, and displacement all start increasing at about $T_1 = 34$ s, which suggests that the slip begins to occur on the fault plane close to this station. The acceleration reaches a maximum at $T_2 = 35.2$ s, and quickly drops to a small value after $T_3 = 36.5$ s, exhibiting an impulsive waveform. In contrast, the velocity reaches the maximum and the displacement keeps increasing until $T_4 = 40$ s. We interpret this as due to widening of the gap and reduction of asperity collisions, as the displacement increases and yields large lubrication pressure. The sudden reduction of very high frequency energy is more obvious on a 5 Hz high-pass filtered accelerogram shown at the bottom of Figure 2. At $T_3 = 36.5$ s, the amplitude on this high-pass filtered record drops abruptly when the displacement is about 4 m and the velocity, 2.5 m/s. A similar behavior can be seen at station TCU052. However, at other stations in the south, we propose that the velocity and displacement did not reach the critical value, and the acceleration kept growing; the acceleration waveforms at these stations are a long wave train in contrast to the spike-like waveforms at stations TCU068 and TCU052 (Figure 1). Figure 1 suggests that the frequency content of the fault motion can be explained by the lubrication mechanism

---

[1] Institute of Geophysics, National Central University, Taiwan.
[2] Department of Earth and Space Sciences, UCLA, USA.
[3] Disaster Prevention Research Institute, Kyoto University, Japan.
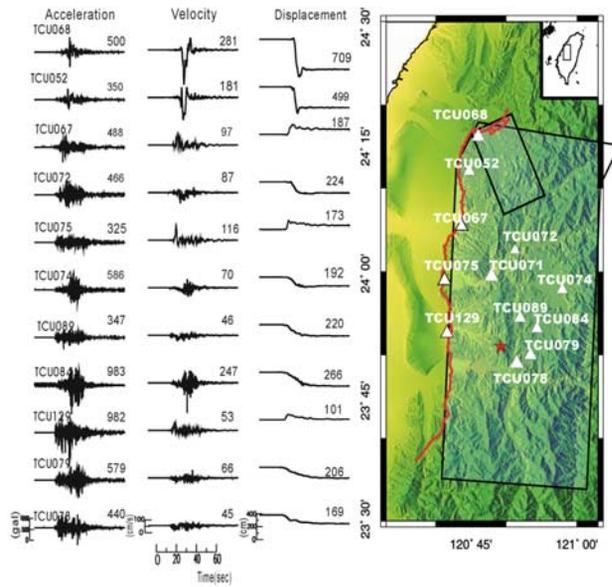[4] Seismological Laboratory, CalTech, Pasadena, USA.

Figure 1. Distribution of the near-field strong-motion stations used in this study (triangles). Shown are east-west components of acceleration, velocity and displacement seismograms for the stations along the fault rupture, and on the hanging-wall of the fault. The number on each seismogram indicates the maximum amplitude in cgs units. The surface breaks of the Chelungpu fault are shown by a bold curve. The blue boxes indicate the geometry used in *Wu et al.* [2001]. The asterisk indicates the epicenter of the 1999 Chi-Chi, Taiwan, earthquake.

although the exact velocity and displacement at which the elastic deformation becomes significant are difficult to predict as the value depend on poorly constrained properties such as viscosity of the fault-zone material, roughness, and the width of the fault zone.

3. Fault Slip Model

[5] Figure 1 shows the ground motion recorded at a station, and is not the slip motion on the fault plane itself. To investigate this problem in further detail, we need to know the temporal and spatial slip distribution on the fault plane. A recent study by *Wu et al.* [2001] modeled the near-source waveforms using a complex fault geometry (Figure 1), which matches the surface rupture of the Chelungpu fault. Figure 3a shows the slip distribution of this model. As shown in *Wu et al.* [2001], this model can explain the observed velocity waveforms at station TCU068 and TCU052 satisfactorily. Most of the slip occurred at shallow depths (0–10 km) in a region north of the hypocenter. To explain the observed waveforms at stations TCU052 and TCU068, large slips are necessary on the NE trending fault segment. These results are similar to other studies [*Ma et al.*, 2001; *Zeng and Chen*, 2001; *Chi et al.*, 2001], regardless of the data and inversion techniques used.

[6] Figure 3b shows the peak slip velocities derived from the temporal and spatial slip distribution. Slip velocities are 0.5–1.0 m/s near the hypocenter and reach larger values of about 2.0 near the surface. The slip velocities in the north, where the fault bends to northeast, reach 3.0–4.5 m/s near

the surface. These values are comparable to the ground-motion velocities observed at the stations located near the surface rupture of the fault. To compare the slip velocities of the slip model with the ground motion velocities observed at the station on the footwall (on the southern portion of the fault), we need to asymmetry of the thrust fault geometry [*Dalguer et al.*, 2001]. The ratio of the ground-motion velocity on the hanging-wall block to that on the footwall block is about 2. If this factor of 2 is taken into account, the spatial slip velocity distribution derived from waveform inversion is consistent with the observed ground-motion velocities, as shown in Figure 3b. The increase of slip velocities from the hypocenter to the region of large slip in the north suggests an increase in dynamic stress drop, which means an increase in the tectonic stress, a decrease in dynamic friction or both during rupture.

4. Lubrication Model

[7] We now interpret the slip distribution shown in Figure 3 using the lubrication model. *Brodsky and Kanamori* [2001] modeled a fault zone as a thin viscous fluid sandwiched between the two walls with undulations having a horizontal length scale *L*. In Brodsky and Kanamori's model, the horizontal length scale develops as the fault slip, d, increases. *Brodsky and Kanamori* [2001] showed that $L \sim d$ on average. The average width of the gap is *H*. Applying the Navier-Stokes equation to this fault zone, i.e., balancing the viscous stresses with a change of pressure in the thin viscous fluid, they obtained as scaling relation for the lubrication pressure P_L given by

$$P_L \approx \frac{6\eta UKL^2}{H^3}, \qquad (1)$$

where η is the viscosity of a slurry of gouge and aqueous fluid, *U* is the fault particle-motion velocity, and *K* is a parameter which represents the roughness. For a general class of self-similar rough surface, $K = \Delta H/L$, where ΔH is the mean amplitude of the undulation of the wall. Fault roughness, *K,* is defined as the ratio of asperity height to asperity length, which has values in the range $10^{-3}-10^{-4}$ [*Power and Tullis*, 1991]. ΔH is assumed to be of the same
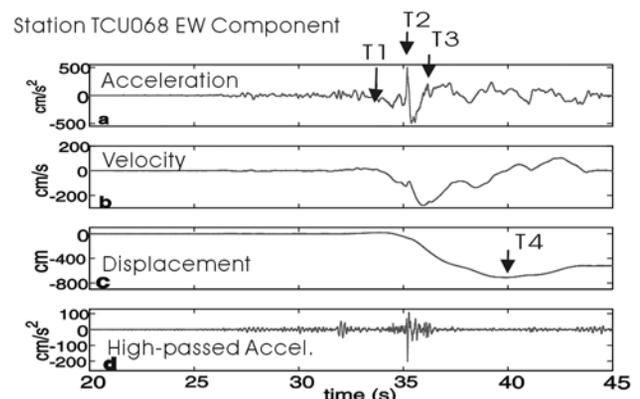

Figure 2. The east-west component of (a) acceleration, (b) velocity, (c) displacement, and (d) 5Hz high-passed acceleration records of station TCU068. The arrows indicate the times at $T_1 = 34$ s, $T_2 = 35.2$s, $T_3 = 36.5$ s and $T_4 = 40$ s.
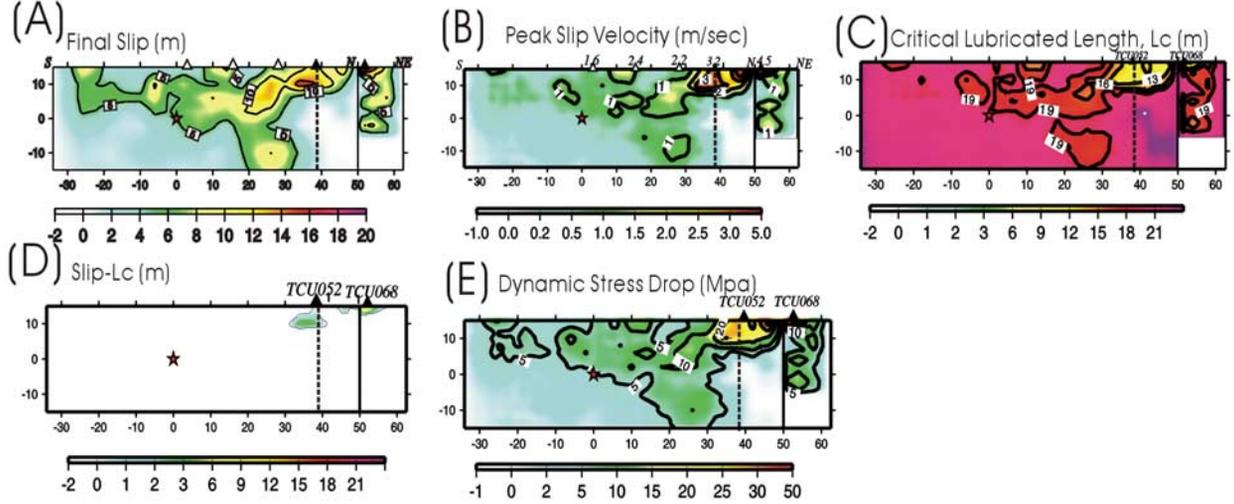
Figure 3. (a) Spatial slip distribution over the fault plane with 5 m intervals. The dashed and solid lines on the fault indicate the fault segments with different fault strikes. The black and white triangles indicate the five stations near the surface breaks on the hanging-wall and footwall, respectively. (b) Peak slip velocity (m/s). The peak slip velocities measured directly from the seismograms at the five stations are given by the numbers next to the station locations. The values for the footwall stations are multiplied by 2 to correct for the difference between hanging-wall and footwall sites. (c) The spatial distribution of calculated critical lubrication length, L_c shown by contour lines (3 m interval). (d) Regions where the total slip, L, shown in Figure 3(a) is larger than L_c Stations.

order as the initial gap height, H_0, i.e., 10^{-3} m. If we include the elastic deformation of the wall, H is given by

$$H = H_0 + \frac{P_L}{E}L \qquad (2)$$

where H_0 is the initial gap, and E is the Young's modulus.

[8] *Brodsky and Kanamori* [2001] defined a critical lubrication length, L_c, below which the elastic contribution to the gap height in equation (2) is insignificant. L_c is defined as the length at which elastic deformation is comparable to the initial gap height, and can be written as

$$L_c = 2H_0 \left(\frac{H_0 E}{6\eta U K} \right)^{1/3} \qquad (3)$$

[9] If $L \ll L_c$, then the elastic deformation of the wall is insignificant; if $L > L_c$, the elastic deformation of the fault wall becomes significant and the gap between the fault walls widens. As the gap widens, the lubrication pressure drops; thus, the gap width will be maintained at an equilibrium value determined by the pressure balance in the gap. The widening reduces the contact area between the asperities on the fault walls and suppresses the radiation of high-frequency energy produced by collision of asperities (Figure 4).

[10] We can calculate L_c over the fault plane from the peak slip velocity obtained from the waveform inversion, using equation (3). For the region where slip is larger than L_c, the fault is pressurized and lubricated. Figure 3c shows the spatial distribution of the critical lubrication length we computed with $E = 5 \times 10^{10}$ Pa, $K = 0.74 \times 10^{-3}$ and $H_0 = 5$ mm. A priori, we can only constrain H_0 to be in the range of millimeters based on geological observations. The specific value of 5 mm is chosen here to provide consistent results with slip inversion. The K value is used for $L = 6.75$ m, which

will be addressed below. In most places, L_c is greater than 10 m, which is larger than the actual slip. Figure 3d shows the region where the critical lubrication length L_c is less than the amount of fault slip and fault lubrication is expected there. The stations TCU068 and TCU052 are located directly above the expected fault lubrication regions. Note that the model predicts only the frequency content of the high slip areas, not their locations. Controlled laboratory experiments at appropriate seismic velocities could help to further asses the importance of lubrication in controlling near field spectral response.

[11] The source time function determined from the waveform inversion indicates that the peak slip velocities are about 3.2 m/s and 4.5 m/s on the subfaults near the station
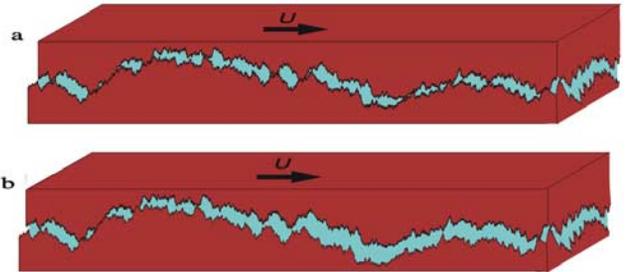

Figure 4. Vertically exaggerated cross-sectional views of the fault zone showing the effect of lubrication on asperities. (a) A fault with low fluid pressure has a significant number of colliding asperities during slip, and radiates significant amounts of high-frequency energy. (b) A lubricated fault has a larger gap between the fault surfaces. Fewer asperities collide during slip, which results in less high frequency radiated energy.

TCU052 and TCU068, respectively. These peak velocities occurred at about 3 sec after the initiation of slip on the subfault. At that moment, the accumulated slips at those subfaults are about 4.8 m and 6.75 m, respectively, and the lubrication pressure is about 20 MPa according to equation (1), with $H_0 = 5$ mm and other parameters as above, i.e. $\eta = 10$ Pa s, $\Delta H \sim H_0 = 0.005$ m ($K = 0.74 \times 10^{-3}$), $U = 4.5$ m/s, $L = 6.75$ m, and $E = 5 \times 10^{10}$ Pa. This lubrication pressure is large enough to increase the average gap by 3 mm according to equation (2), i.e., from 5 to 8 mm. For a typical fault roughness of $K = 10^{-3} - 10^{-4}$, the widening of the gap will result in a smaller surface area of asperity contact. The reduced number of asperities in contact suppresses the radiation of high frequency energy at stations TCU052 and TCU068 (Figure 1). In contrast, the slip near the epicenter was not large enough to increase the pressure to widen the fault gap. The asperities in the fault gap were almost fully in contact and generated high frequency energy as observed (Figure 1) at the stations near the epicenter. Since the model parameters, such as H_0 and ΔH, are only constrained to within an order of magnitude in the absence of direct observations, such as those from fault core samples, it is unlikely that a single observation exactly matches the values given above. In view of these uncertainties, we emphasize here the qualitative prediction of the lubrication model rather than the specific numerical results.

[12] Lubrication in the large slip region increases the fluid pressure by 20 MPa. For a typical frictional coefficient (μ_s) of $0.5 - 0.7$, this corresponds to an increase in the shear stress driving fault motion by $10 - 14$ MPa. Simple crack models suggest an increase of slip velocity of approximately 1 m/s for an increase in the stress of 10 MPa [*Brune*, 1970]. The large slip velocity, $3.2 - 4.5$ m/s, observed in the northern part is about $1 - 2$ m/sec larger than that in the south, which is consistent with the locally increased driving stress.

5. Discussion and Conclusions

[13] Given the consistency between the data and predictions of lubrication model shown above, we suggest the following rupture model. The rupture initiated at the hypocenter and propagated to the north. As the fault slipped, lubrication pressure increased, which reduced the frictional stress. The asperities on the fault walls were initially in full contact, but as the lubrication pressure widened the fault gap, the area of asperity contact decreased which decreased the radiation of high frequency accelerations. A consequence was reduced shaking damage on small structures in the area, despite the large slip and slip velocity.

[14] The lubrication model provides a quantitative model for the rupture behavior of the Chi-Chi earthquake, as shown above, that successfully predicts the area of reduced high frequency radiation and the distribution of dynamic stress drop with a priori chosen parameter H_0. Other mechanisms such as melting and fluid pressurization may have similar effects on rupture dynamics, as discussed in *Kanamori and Heaton* [2000]. Also, the difference in the properties of fault-zone materials between north and south

may also be responsible for the difference in rupture behavior. These can be examined by the possible future drilling of Chelungpu fault.

[15] High-frequency (>1 Hz) seismic waves attenuate quickly. Before 1999, no earthquake with large slip (>10 m) had more than one seismic station within 2 wavelengths (10 km) of the rupture. Therefore, the lubrication effect may not have been obvious for other earthquakes in the past. The result from the 1999 Chi-Chi earthquake suggests that if slip exceeds a critical value, the fault lubrication may cause even larger slip and higher slip velocity due to the reduction of friction. Thus, the ground motions of large earthquakes cannot be estimated by simple scaling of smaller earthquakes. Since long-period ground-motions can significantly influence large buildings and structures, dynamic effects such as lubrication should be carefully considered in future designs of large structures.

References

Brodsky, E. E., and H. Kanamori, Elastohydrodynamic lubrication of faults, *J. Geophys. Res.*, *106*, 16,357–16,374, 2001.

Brune, J. N., Tectonic stress and the spectra of seismic shear waves from earthquakes, *J. Geophys. Res.*, *75*, 4997–5009, 1970.

Chi, W.-C., D. Dreger, and A. Kaverina, Finite-source modeling of the 1999 Taiwan (Chi-Chi) earthquake derived from a dense strong-motion network, *Bull. Seismol. Soc. Am.*, *91*, 1144–1157, 2001.

Dalguer, L. A., K. Irikura, J. D. Riera, and H. C. Chiu, The importance of the dynamic source effects on strong ground motion during the 1999 Chi-Chi, Taiwan, earthquake: Brief interpretation of damage distribution on buildings, *Bull. Seismol. Soc. Am.*, *91*, 1112–1127, 2001.

Fukuyama, E., and R. Madariaga, Rupture dynamics of a planar fault in a 3D elastic medium: Rate- and slip-weakening friction, *Bull. Seismol. Soc. Am.*, *88*, 1–17, 1998.

Kanamori, H., and T. H. Heaton, Microscopic and macroscopic physics of earthquakes, in *GeoComplexity and the Physics of Earthquakes*, Geophys. Monogr. Ser., vol. 120, edited by J. B. Rundle, D. L. Turcotte, and W. Klein, pp. 147–183, AGU, Washington, D. C., 2000.

Ma, K. F., J. Mori, S. J. Lee, and S. B. Yu, Spatial and temporal distribution of slip for the 1999 Chi-Chi, Taiwan, earthquake, *Bull. Seismol. Soc. Am.*, *91*, 1069–1087, 2001.

Power, W. L., and T. E. Tullis, Euclidean and fractal models for the description of rock surface roughness, *J. Geophys. Res.*, *93*, 415–424, 1991.

Sommerfeld, A., *Mechanics of Deformable Bodies*, 396 pp., Academic, San Diego, Calif., 1950.

Wu, C., M. Takeo, and S. Ide, Source process of the Chi-Chi earthquake: A joint inversion of strong motion data and global positioning system data with multifault model, *Bull. Seismol. Soc. Am.*, *91*, 1128–1143, 2001.

Zeng, Y., and C.-H. Chen, Fault rupture process of the 20 September 1999 Chi-Chi, Taiwan, earthquake, *Bull. Seismol. Soc. Am.*, *91*, 1088–1098, 2001.

————————

E. E. Brodsky, Department of Earth and Space Sciences, University of California, Los Angeles, CA 90024, USA.

C. Ji, H. Kanamori, and T.-R. A. Song, Seismological Laboratory, California Institute of Technology, Pasadena, CA 91125, USA. (jichen@gps.caltech.edu; hiroo@seismo.gps.caltech.edu)

K.-F. Ma, Institute of Geophysics, National Central University, Chung-li 320-54, Taiwan. (fong@rupture.gep.ncu.edu.tw)

J. Mori, Disaster Prevention Research Institute, Kyoto University, Gokasho, Uji, Kyoto 611-0011, Japan. (mori@rcep.dpri.kyoto-u.ac.jp)